Vol 17 No 6, June 2008
1674-1056/2008/17(06)/2116-08

Chinese Physics B

A density functional theoretical investigation of $RhSi_n(n = 1–6)$ clusters*

Ren Zhao-Yu(任兆玉)[a)†], Hou Ru(侯 茹)[a)b)], Guo Ping(郭 平)[c)], Gao Ji-Kai(高继开)[a)], Du Gong-He(杜恭贺)[a)], and Wen Zhen-Yi(文振翼)[d)]

[a)] *Institute of Photonics & Photon-Technology, Northwest University, Xi'an* 710069, *China*
[b)] *Physics Department of Shangluo University, Shangluo* 726000, *China*
[c)] *Physics Department of Northwest University, Xi'an* 710069, *China*
[d)] *Institute of Modern Physics, Northwest University, Xi'an* 710069, *China*

(Received 31 May 2007; revised manuscript received 23 October 2007)

This paper computationally investigates the $RhSi_n(n = 1–6)$ clusters by using a density functional approach. Geometry optimizations of the $RhSi_n(n = 1–6)$ clusters are carried out at the B3LYP level employing LanL2DZ basis sets. It presents and discusses the equilibrium geometries of the $RhSi_n(n = 1–6)$ clusters as well as the corresponding averaged binding energies, fragmentation energies, natural populations, magnetic properties, and the energy gaps between the highest occupied molecular orbital and the lowest unoccupied molecular orbital. Theoretical results show that the most stable $RhSi_n(n = 1–6)$ isomers keep an analogous framework of the corresponding Si_{n+1} clusters, the $RhSi_3$ is the most stable cluster in $RhSi_n(n = 1–6)$ isomers. Furthermore, the charges of the lowest-energy $RhSi_n(n = 1–6)$ clusters transfer mainly from Si atom to Rh atom. Meanwhile, the magnetic moments of the $RhSi_n(n = 1–6)$ arises from the 4d orbits of Rh atom. Finally, compared with the Si_{n+1} cluster, the chemical stability $RhSi_n$ clusters are universally improved.

Keywords: density functional theory, $RhSi_n$ clusters, geometrical stability
PACC: 3640, 3640B, 3640C

1. Introduction

Atomic clusters represent a new phase of matter between molecules and solids, the chemical and physical properties of a cluster are different from the properties of the component atoms/molecules or of the extended bulk material.[1] The Si clusters have been extensively investigated both experimentally and theoretically because silicon is an important semi-conducting element in microelectronics industry. However, because the lack of sp^2 hybridization in silicon clusters, pure silicon clusters are unfavorable to form a fullerene cage and exhibit instability.[2,3] A feasible way which can improve stability of the Si clusters is to locate a guest atom in the Si_n clusters. Beck[4] pioneered the synthesis of the different-sized MSi_n (M = Cr, Mo, W, etc.) clusters through the laser photoionization coupled with the time-of-flight mass spectrometry technique and revealed that the metal-doped silicon clusters were more stable towards photofragmentation than the bare silicon clusters with the same size. Subsequently, Hiura *et al*[5] used an external quadrupole static attraction ion trap to produce transition metal (TM)-dependent-sized $MSi_nH_x^+$ and MSi_n^+ clustered ions. Stimulated by these experimental results, the transition metal silicon clusters had been extensively investigated both theoretically and experimentally.[6–8] These investigations indicate that the TM doped silicon cluster is a semiconducting cluster which is great important for applications in microelectronic technology and material science. In addition, the TM clusters have a variety of special properties, such as superconductive, nonlinear optical properties and so on, which are distinguished from other clusters and material structure.[9,10] Therefore, the investigations of the equilibrium geometries, stabilities, and electronic properties of these clusters are practically significant.

The rhodium (Rh) element in TM is found in VIIIA group of the periodic table, with an electronic configuration $4d^85s^1$. The incomplete d subshell and d electrons are responsible for its most interesting prop-

*Project supported by the National Natural Science Foundation of China (Grant No 10247007), the Natural Science Foundation of Shaanxi Province (Grant No 2002A09), and the Special Item Foundation of Educational Committee of Shaanxi Province (Grant No 02JK050).
†E-mail: rzy@nwu.edu.cn

erties as free atoms or in metallic bulk phase. The RhC, RhN, RhH, $RhCH_3$, RhHCO, $Rh(CO_2)$, and $Rh_n(n = 2-13)$ clusters have been investigated.[11−13] However, there are no systematic investigation of $RhSi_n(n = 1–6)$ clusters within density functional theory (DFT) approach considering exchange-correlation functional. The main objective of these studies, therefore, is to provide theoretical understanding and interpreting of the geometries, relative stabilities and charge-transfer mechanisms of the rhodium silicone clusters.

2. Computational details

All computations are carried out by using the GAUSSIAN 03 program package.[14] The geometry optimizations of $RhSi_n(n = 1–6)$ clusters with doublet, quartet, and sextet configurations are performed by DFT at the UB3LYP[15,16] level employing the effective core potential (ECP) LanL2DZ (Stuttgart/Dresden effective core potential) basis sets,[17] which provide an effective way to reduce difficulties in the calculations of two-electron integrals caused by a heavy TM atom. The LanL2DZ basis sets are proven to be reliable for the geometries, stabilities, and electronic properties of $TM@Si_n$ systems.[6,9,18−22]

To check the reliability of our calculations, the Si_2 and Rh_2 dimers are calculated. The calculated results show that the triplet Si_2 is the most stable structure. The calculated Si–Si bond length 2.352Å and the Rh–Rh bond length 2.321Å is in good agreement with the experimental values of 2.246Å [23] and 2.28Å,[24] respectively. Consequently, the B3LYP/ LanL2DZ method is reliable and accurate enough to describe the properties of $RhSi_n$ clusters. For each stationary point of cluster, the stability is examined by the harmonic vibration frequency calculation. When an imaginary frequency is found, a relaxation along the coordination of the imaginary vibration mode is carried out until a true minimum occurs. Therefore, all clusters are fully optimized and their equilibrium geometries and total energies are surely the stable structures and local minimum.

3. Results and discussions

3.1. Geometry and stability

The calculated results of bond length and bond angle, total energy, together with the electronic state are listed in Table 1. The geometrical structures are displayed in Fig.1.

3.1.1. RhSi

The RhSi cluster with the electron spins $S = 1/2$, 3/2, and 5/2 is optimized and the corresponding ground state configuration is listed in Fig.1. The total energies of the RhSi clusters with spin $S = 1/2$, 3/2, and 5/2 are −113.3182, −113.2947, −113.2383 hartree, respectively. The doublet spin configuration is more stable than the quartet and the sextet by the energy differences of 0.6395 and 2.1742 eV, respectively. Therefore, the RhSi cluster with spin $S = 1/2$ is the most stable structure and is selected as the ground state, and the corresponding electronic state is $^2\Sigma_g$. The spin configuration of the most stable RhSi cluster is similar to those of the IrSi.[6] Furthermore, the Rh–Si bond length of the RhSi cluster is 2.1146, 2.2391, and 2.4627Å, respectively for $S = 1/2$, 3/2, and 5/2, and it obviously depends on spin configuration.

The Rh–Si bond length (2.115Å) of RhSi is shorter than the Si–Si bond length (2.352 Å) of Si_2 at the same level of theory, and the corresponding binding energy (1.6089 eV) is smaller than that (3.30 eV) of Si_2, indicating that the Rh–Si interaction is weaker than the Si-Si interaction. Therefore, the Si-Si interaction may determine the equilibrium geometry of the $RhSi_n(n = 1–6)$. This feature is similar to those of $CuSi_n$ clusters[7] and $TaSi_n$ clusters.[8]

3.1.2. $RhSi_2$

All the possible geometries of the $RhSi_2$ cluster, maintaining C_{2v}, $C_{\infty v}$, and $D_{\infty h}$ symmetries, are considered. The isosceles-triangle C_{2v} and the linear $C_{\infty v}$ structures with electron spin configurations of $S = 1/2$, 3/2, and 5/2 are all proved to be stable geometries, but the $D_{\infty h}$ structure with various spin configurations are turned out not to be equilibrium geometry. However, the C_{2v} symmetry isosceles-triangle with spin $S = 1/2$, 3/2, and 5/2, are lower than the linear $C_{\infty v}$ structure same spin configurations in energy. So the linear structure is less stable than the triangle planar structure. The spin quartet geometry of this C_{2v} symmetry is a lowest-energy configuration; the corresponding electron state is $^4B_1$. As seen from Table 1, the bond lengths of $RhSi_2$ (C_{2v}, $C_{\infty v}$) isomers also obviously depend on the spin. When spin goes from $S = 1/2$, 3/2, to 5/2, Rh–Si bond lengths (R_1) increase monotonically.

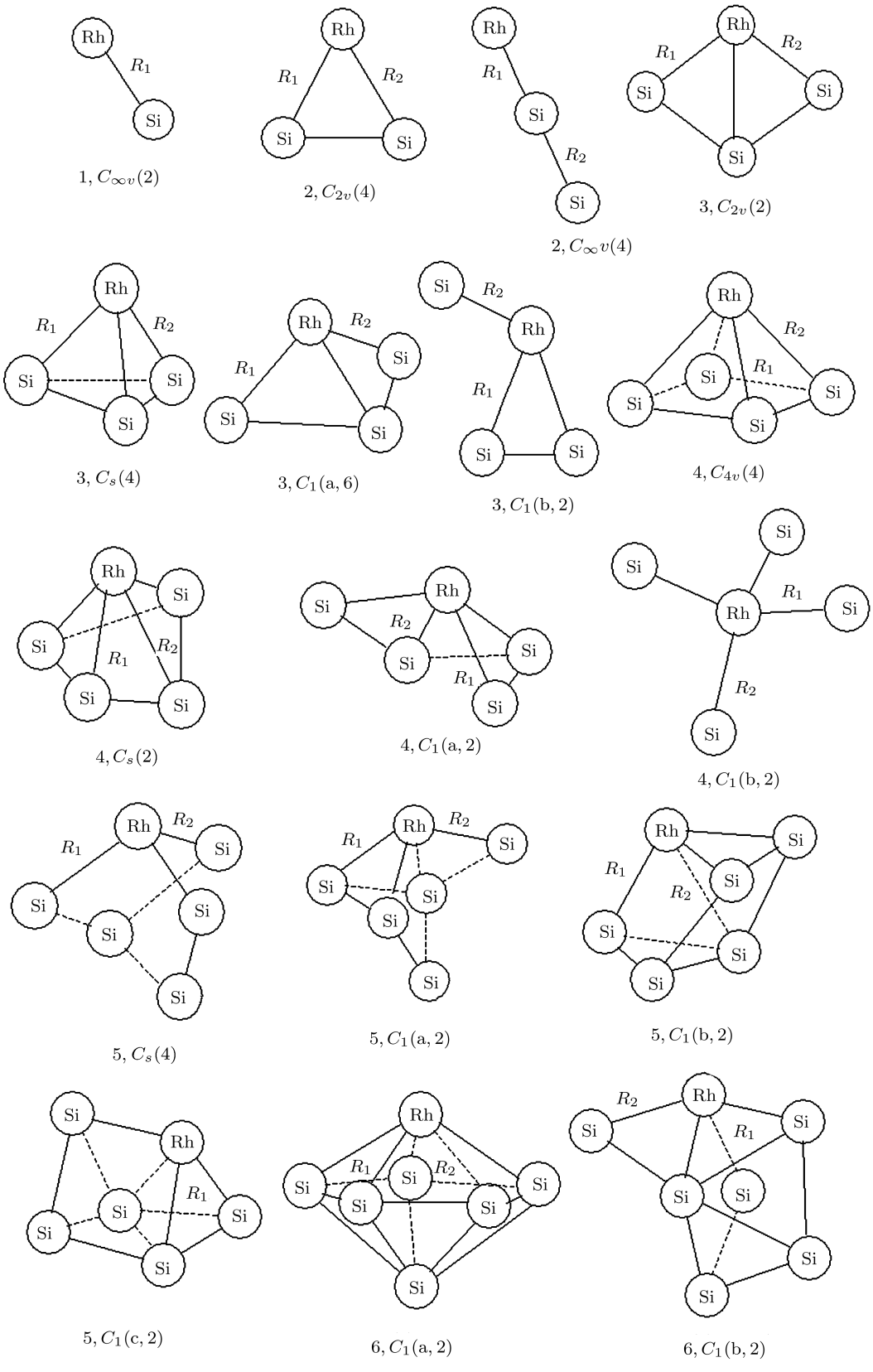

Fig.1. Structures of the most stable $RhSi_n (n = 1–6)$ clusters.

Table 1. Geometries, total energies and electronic state of $RhSi_n(n = 1–6)$ clusters.

Cluster	Sym	Spin	R_1	R_2	Si(1)RhSi(2)	E_b	state
RhSi	$C_{\infty v}$	1/2	2.1146			–113.3182	$^2\Sigma_g$
		3/2	2.2391			–113.2947	
		5/2	2.4627			–113.2383	
$RhSi_2$	C_{2v}	1/2	2.2639	2.2639	63.3641	–117.1924	$^2B_1$
		3/2	2.3491	2.3491	60.3664	–117.19528	$^4B_1$
		5/2	2.4642	2.4642	61.6951	–117.09424	$^6B_1$
	$C\infty v$	1/2	2.1634	2.3519	180	–117.1255	^2B
		3/2	2.1895	2.2798	180	–117.15306	$^4\Sigma_g$
		5/2	2.3923	2.2496	180	–117.0278	$^6\Sigma_g$
	$D_{\infty H}$	5/2	2.285	2.285	180	–116.9265	TS $^6\Sigma_g$
$RhSi_3$	C_{2v}	1/2	2.3115	2.3115	111.0273	–121.09598	$^2B_1$
		3/2	2.2781	3.1282	100.7055	–121.0562	$^4B_1$
		5/2	2.3366	2.3366	88.2004	–120.9981	TS $^6A_1$
	C_s	1/2	2.314	2.4223		–121.0701	TS $^2A'$
		3/2	2.3859	2.3856		–121.0741	$^4A''$
		5/2	2.3021	2.2959	100.0808	–121.0050	TS$^6A''$
	C_1(a)	1/2	2.3119	2.3119	111.0048	–121.0960	^2A
		3/2	2.2783	2.2781	100.7044	–121.0562	^4A
		5/2	2.3097	2.3097	111.3099	–121.0107	^6A
	C_1(b)	1/2	2.3739	2.1993	105.8171	–121.0620	^2A
		3/2	2.2369	2.2368	98.6107	–121.0491	^4A
$RhSi_4$	C_{4v}	1/2	2.5871	2.5871	83.4721	–124.9113	$^2B_1$
		3/2	2.4957	2.4957	88.4521	–124.9313	$^4A_1$
		5/2	2.376	2.6287		–124.8969	
	C_{3v}	1/2	2.2205	2.2416	113.0084	–124.9227	^2A
	C_s	1/2	2.4287	2.7663	103.719	–124.9580	$^2A''$
		3/2	2.3776	3.0733	101.5956	–124.9387	TS $^4A''$
	C_1	1/2	2.3067	2.7345	90.0059	–124.9552	^2A
		3/2	2.3403	2.8078	80.8014	–124.9412	^4A
		5/2	2.3766	2.3773	93.0781	–124.8969	^6A
$RhSi_5$	C_s	1/2	2.3441	2.4052	130.7327	–128.7917	$^2A'$
		3/2	2.3229	2.3229	103.4113	–128.8143	$^4A''$
		5/2	2.268	2.3998	129.9643	–128.7462	$^6A''$
	C_1(a)	1/2	2.4442	2.309	108.9145	–128.8378	^2A
		3/2	2.3489	2.3117	102.9596	–128.8139	^4A
		5/2	2.417	2.417	101.1195	–128.7777	^6A
	C_1(b)	1/2	2.3282	2.7307	113.1515	–128.8347	^2A
	C_1(c)	1/2	3.1569	2.4455	94.378	–128.8347	^2A
$RhSi_6$	C_s	1/2	2.4926	2.3611	117.3568	–132.6665	$^2A'$
		3/2	2.4743	2.3227	161.6777	–132.6518	TS $^4A''$
		5/2	2.421	2.419	92.9508	–132.6174	$^6A'$
	C_1(a)	1/2	2.5325	2.5314	104.4966	–132.7129	^2A
		3/2	2.9357	2.4007	88.6922	–132.69329	^4A
		5/2	3.1244	2.3769	62.6897	–132.6568	^6A
	C_1(b)	1/2	2.295	2.3489	105.7471	–132.7030	^2A
		3/2	2.3234	2.4098	103.6698	–132.6818	^4A
		5/2	2.2976	2.4757	117.8554	–132.6607	^6A

3.1.3. $RhSi_3$

For $RhSi_3$ clusters, the initial structures optimized are the C_{2v}, planar rhombus and C_{3v} trigonal pyramid. As a result, we get a stable C_{2v} symmetry rhombus and three distortions of the C_{3v} trigonal pyramid, a C_s symmetry, a kite-like C_1(a) symmetry, and a scoop-like C_1(b) symmetry. The C_{2v} structures with doublet and quartet spin configurations are proven to be stable geometry, but its sextet spin configuration has one imaginary frequency. The Rh-capped C_s symmetry structure with doublet and sextet spin configurations are not the stable structures, except its quartet spin configuration. The C_1(a) clusters with $S = 1/2$, $3/2$, and $5/2$ as well as the C_1(b) clusters with $S = 1/2$ and $3/2$ are the stable structures. As seen from Table 1, the C_{2v} symmetry $RhSi_3$ ($S = 1/2$) with the corresponding electronic state $^2B_1$ is the lowest-energy structure, which is analogy to the previous optimization results of the $IrSi_3$[6] and keeps the same frame of Si_4 clusters.[10] In a word, it is the tridimensional structure that is more stable than the plane and linear geometry for $RhSi_3$ cluster, which is different from RhC_3 cluster.[25]

3.1.4. $RhSi_4$

The possible low-lying $RhSi_4$ isomers are identified as the tetragonal pyramid C_{4v} structure, the tetragonal pyramid C_s structure, and the butterfly-like C_1(a) structure (Fig.1). Theoretical results reveal that the C_{4v} and the C_1(a) structures with doublet, quartet, and sextet spin states, as well as the C_s structure with only spin $S = 1/2$ are stable structure. On the basis of total energies, it is obvious that $RhSi_4$ (C_s with spin doublet configuration is the lowest-energy configuration with electron state $^2A''$, and the most stable $RhSi_4$ structure basically keeps the same framework as the Si_5 clusters.

3.1.5. $RhSi_5$

The four $RhSi_5$ isomers are acquired by optimizing the possible initial geometries. They are depicted as the distorted tetragonal bipyramid structure (C_s), the distorted tetragonal bipyramid C_1(a) structure, and the distorted trigonal prism with C_1 symmetries (Fig.1). Although the C_s isomers with spin $S = 1/2$, $3/2$, and $5/2$ are stable structures, the relaxed C_1(a) isomer with various spin states has lower energy, and its spin doublet state is a lowest-energy configuration with electron state ^2A. The lowest-energy $RhSi_5$ isomer also maintains the same framework as the Si_6 clusters.

3.1.6. $RhSi_6$

Guided by the previous theoretical results of $TaSi_6$ clusters,[7] we only consider the pentagonal bipyramid and the edge-capped trigonal prism (Fig.1). Theoretical results show that the two structures with spin $S = 1/2$, $3/2$, and $5/2$ are indeed local minimum on the potential energy surface, however, they are optimized into a low symmetry C_1(a) structure and C_1(b) structure. The pentagonal bipyramid C_1(a) structure with doublet spin configuration has the lowest energy, whose structure is similar to the most stable structure of Si_7 clusters.

3.2. Binding energies and fragmentation energies

In order to investigate the relative stability of the most stable $RhSi_n (n = 1–6)$ clusters, it is significant to calculate the atomic averaged binding energies ($E_b(n)$) and fragmentation energies ($D(n, n-1)$) with respect to the isolated atoms. The atomic averaged binding energies and fragmentation energies of the $RhSi_n (n = 1–6)$ clusters are defined as:

$$E_b(n) = [nE_T(Si) + E_T(Rh) - E_T(RhSi_n)]/(n+1),$$

$$D(n, n-1) = E_T(RhSi_{n-1}) + E_T(Si) - E_T(RhSi_n).$$

Where $E_T(RhSi_{n-1})$, $E_T(Si)$, $E_T(Rh)$, and $E_T(RhSi_n)$ are the total energies of the most stable $RhSi_{n-1}$, Si, Rh, and $RhSi_n$ clusters, respectively. Size dependence of the atomic averaged binding energies and the fragmentation energies of the most stable $RhSi_n (n = 1–6)$ clusters are displayed in Fig.2. Our calculated results for $E_b(1)$, $E_b(2)$, $E_b(3)$, $E_b(4)$, $E_b(5)$, $E_b(6)$ are 1.6089, 2.1023, 2.5099, 2.5439, 2.6473, and 2.7032 eV, respectively. As seen from Fig.2, the binding energies of $RhSi_n$ clusters increase with the number of Si atoms, the peak is found at $n = 3$, indicating that $RhSi_3$ cluster is relatively more stable. For the fragmentation energies $D(n, n-1)$, the calculated results are 3.0893, 3.7327, 2.6798, 3.1643, and 3.0383 eV respectively for $D(2, 1)$, $D(3, 2)$, $D(4, 3)$, $D(5, 4)$, and $D(6, 5)$, and the $D(3, 2)$ is the largest, as seen from Fig.3, which further indicates that the $RhSi_3$ cluster is more stable than the $RhSi_n (n = 1, 2, 4–6)$ clusters with respect to the removal of one silicon atom.

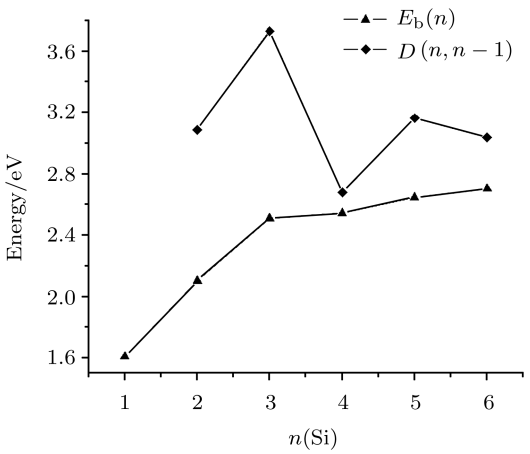

Fig.2. The size dependence of atomic averaged binding energies ($E_b(n)$) and fragmentation energies ($D(n, n-1)$) of the lowest-energy Rhsin clusters.

3.3. Population analyses

The natural populations and natural electron configurations of the most stable $RhSi_n(n = 1–6)$ clusters are summarized in Table 2. The natural populations of Rh $RhSi_n(n = 1–6)$ isomers are negative except $RhSi_2$, indicating that charges are transferred from silicon atoms to Rh atom. This finding on charge-transfer is similar to the MSi_n (M = Cr, Mo, W, Ir; $n = 1–6$) clusters.[19,22] The charges transfer from Si atom to 5s orbital and 4d orbitals of Rh. As seen from Table 2, more than 8.4 electrons occupy the 4d subshell of Rh in $RhSi_n$, indicating that the 4d orbital of Rh atom in $RhSi_n(n = 1–6)$ does behave as a core orbital and take an active role in the bonding.

Table 2. Natural populations and natural electron configurations of the lowest-energy $RhSi_n(n = 1–6)$ clusters.

System	Symm	Spin	Atom	Natural population	Natural electron configuration
RhSi	$C_{\infty v}$	1/2	Rh	–0.38610	[core]$5s^{0.54}4d^{8.85}5p^{0.01}$
			Si	0.38610	[core]$3s^{1.92}3p^{1.69}$
$RhSi_2$	C_{2v}	3/2	Rh	0.02583	[core]$5s^{0.46}4d^{8.49}5p^{0.03}5d^{0.01}$
			Si_1	–0.01291	[core]$3s^{1.80}3p^{2.21}4p^{0.01}$
			Si_2	–0.01291	[core]$3s^{1.80}3p^{2.21}4p^{0.01}$
$RhSi_3$	C_{2v}	1/2	Rh	–0.11209	[core]$5s^{0.34}4d^{8.74}5p^{0.04}5d^{0.01}$
			Si_1	–0.22231	[core]$3s^{1.59}3p^{2.61}4p^{0.01}$
			Si_2	0.16720	[core]$3s^{1.79}3p^{2.04}$
			Si_3	0.16720	[core]$3s^{1.79}3p^{2.04}$
$RhSi_4$	C_s	1/2	Rh	–0.16316	[core]$5s^{0.30}4d^{8.81}5p^{0.01}$ $^{0.05}$5d
			Si	0.08633	[core]$3s^{1.76}3p^{2.15}4p^{0.01}$
			Si	–0.10807	[core]$3s^{1.60}3p^{2.49}4p^{0.01}$
			Si	0.09857	[core]$3s^{1.82}3p^{2.07}4p^{0.01}$
			Si	0.08633	[core]$3s^{1.76}3p^{2.15}4p^{0.01}$
$RhSi_5$	C_1(a)	1/2	Rh	–0.27066	[core]$5s^{0.37}4d^{8.85}5p^{0.06}5d^{0.01}$
			Si	0.01757	[core]$3s^{1.69}3p^{2.28}4p^{0.01}$
			Si	0.10600	[core]$3s^{1.73}3p^{2.15}4p^{0.01}$
			Si	0.29269	[core]$3s^{1.77}3p^{1.93}4p^{0.01}$
			Si	–0.19772	[core]$3s^{1.56}3p^{2.63}4p^{0.01}$
			Si	0.05212	[core]$3s^{1.72}3p^{2.22}4p^{0.01}$
$RhSi_6$	C_1(a)	1/2	Rh	–0.24761	[core]$5s^{0.32}4d^{8.84}5p^{0.10}5d^{0.01}$
			Si	0.05057	[core]$3s^{1.68}3p^{2.26}4p^{0.01}$
			Si	0.05076	[core]$3s^{1.68}3p^{2.26}4p^{0.01}$
			Si	0.05053	[core]$3s^{1.68}3p^{2.26}4p^{0.01}$
			Si	0.05097	[core]$3s^{1.68}3p^{2.26}4p^{0.01}$
			Si	0.05062	[core]$3s^{1.68}3p^{2.26}4p^{0.01}$
			Si	–0.00584	[core]$3s^{1.65}3p^{2.34}4p^{0.01}$

3.4. Magnetic properties

Table 3 lists spin net populations γ of Rh atom, spin densities (d(4d)) of 4d orbit, and averaged magnetic moment δ in the most stable $RhSi_n(n = 1–6)$ clusters. Where $\gamma = |\alpha - \beta|$, averaged magnetic moment: $\delta = 2S/n + 1$. The magnetic moment is proportional to the γ. As seen from Table3, the values of γ $RhSi_n(n = 1–6)$ are universally bigger than that of averaged magnetic moment (δ), indicating that the magnetic moment of $RhSi_n$ clusters mainly raises from 4d orbital of Rh atom and have been passivated by Si atoms.

Table 3. Natural spin population of Rh atom, spin density of 4d orbit and averaged magnetic moment of the lowest-energy $RhSi_n(n = 1–6)$ clusters.

Cluster	Symm	Spin	α	β	γ	d(4d)	$\delta(\mu_b)$
RhSi	$C_{\infty v}$	1/2	–0.51793	0.13183	0.64976	0.23	0.50
$RhSi_2$	C_{2v}	3/2	–0.65591	0.68174	1.33765	1.21	1.00
$RhSi_3$	C_{2v}	1/2	–0.34751	0.23542	0.58293	0.47	0.25
$RhSi_4$	C_s	1/2	–0.27973	0.11657	0.3963	0.40	0.20
$RhSi_5$	C_1(a)	1/2	–0.29393	0.02327	0.3172	0.26	0.17
$RhSi_6$	C_1(a)	1/2	–0.29134	0.04374	0.33508	0.24	0.14

3.5. HOMO–LUMO gaps

The electronic properties of $RhSi_n$ clusters can be reflected by the energy gap between the highest occupied molecular orbital (HOMO) and the lowest unoccupied molecular orbital (LUMO). The HOMO–LUMO gaps of the lowest-energy $RhSi_n$ clusters are listed in Table 4. The HOMO–LUMO gaps of the $RhSi_n$ clusters are generally larger than that of the pure Si_{n+1} cluster, indicating that their chemical stability is improved. The $RhSi_2$ has the smallest HOMO–LUMO gaps, while the $RhSi_3$ cluster has the largest one, which further proves that the $RhSi_3$ cluster has enhanced stability.

Table 4. The HOMOs, LUMOs and HOMO–LUMO gaps of the lowest-energy $RhSi_n(n = 1–6)$ clusters.

System	Sym	Spin	α–HOMO	α–LUMO	β–hOMO	β–LUMO	E_{gap}/ev
RhSi	$C_{\infty}v$	1/2	–0.18256	–0.09591	–0.19520	–0.11019	1.96846
$RhSi_2$	C_{2v}	3/2	–0.20497	–0.08383	–0.24500	–0.14214	1.70898
$RhSi_3$	C_{2v}	1/2	–0.21722	–0.11987	–0.22586	–0.14094	2.07482
$RhSi_4$	C_s	1/2	–0.21779	–0.13571	–0.21420	–0.14716	1.82349
$RhSi_5$	C_1(a)	1/2	–0.21050	–0.13122	–0.21757	–0.14643	1.74270
$RhSi_6$	C_1(a)	1/2	–0.22820	–0.13986	–0.23132	–0.16359	1.75739

4. Conclusion

The $RhSi_n(n = 1–6)$ clusters with doublet, quartet, and sextet spin configurations are investigated at the (U) B3LYP level using LanL2DZ basis set. The total energies, equilibrium geometries, and stabilities of $RhSi_n(n = 1–6)$ clusters, together with fragmentation energies and atomic averaged binding energies as well as natural populations and natural electron configurations, are presented and discussed. Theoretical results reveal that the lowest-energy $RhSi_n$ structures basically maintain the same framework as Si_{n+1} and correspond to the spin doublet configuration except $RhSi_2$. The discussions on atomic averaged binding energy and fragmentation energy show that the lowest-energy $RhSi_3$ cluster has enhanced stability in $RhSi_n(n = 1–6)$ clusters. The analysis of natural population and natural electron configurations indicate that the charges transfer from Si atoms to 4d orbital of Rh atom, and Rh atom acts as an acceptor. The analyses of magnetic properties indicate that the magnetic moment of the $RhSi_n(n = 1–6)$ clusters comes mainly from 4d orbital of Rh atom. Finally, the analyses of HOMO–LUMO gaps show that the chemical stability of the $RhSi_n$ clusters is improved relative to the corresponding pure Si_{n+1} clusters.

References

[1] Zhang C R, Chen H S, Song Y and Xu G J 2007 *Chin. Phys.* **16** 2394

[2] Ho K M, Shvartsburg A A, Pan B, Lu Z Y, Wang C Z, Wacker J G, Fye J and Jarrold M F 1998 *Nature* (London) **392** 582

[3] Rata I, Shvartsburg A A, Horoi M, Frauenheim T, Michael Siu K W and Jackson K A 2000 *Phys. Rev. Lett.* **85** 546

[4] Hiura H, Miyazaki T and Kanayama T 2001 *Phys. Rev. Lett.* **86** 1733

[5] Han J G 2003 *Chem. Phys.* **286** 181

[6] Xiao C, Hageberg F, Ovcharenko I and Lester W A 2001 *J. Mol. Struct.* : *THEOCHEM* **549** 181

[7] Guo P, Ren Z Y, Wang F, Bian J and Han J G 2004 *J. Chem. Phys.* **121** 20

[8] Han J G, Ren Z Y and Lu B Z 2004 *J. Phys. Chem.* A **108** 5100

[9] Han J G 2000 *Chem. Phys. Lett.* **324** 143

[10] Tan H, Liao M Z and Balasubramanian K 1997 *Chem. Phys. Lett.* **280** 423

[11] Irene S, Kim M and Karl A G 1997 *Theo. Chem.* **393** 127

[12] Reddy B V, Nayak S K, Khanna S N, Rao B K and Jena P 1998 *Phys. Rev.* B **59** 5214

[13] Frisch M J, Trucks G W, Schlegel H B, Scuseria G E, Robb M A, Cheeseman J R, Montgomery J A Jr, Vreven T, Kudin K N, Burant J C, Millam J M, Iyengar S S, Tomasi J, Barone V, Mennucci B, Cossi M, Scalmani G, Rega N, Petersson G A, Nakatsuji H, Hada M, Ehara M, Toyota K, Fukuda R, Hasegawa J, Ishida M, Nakajima T, Honda Y, Kitao O, Nakai H, Klene M, Li X, Knox J E, Hratchian H P, Cross J B, Bakken V, Adamo C, Jaramillo J, Gomperts R, Stratmann R E, Yazyev O, Austin A J, Cammi R, Pomelli C, Ochterski J W, Ayala P Y, Morokuma K, Voth G A, Salvador P, Dannenberg J J, Zakrzewski V G, Dapprich S, Daniels A D, Strain M C, Farkas O, Malick D K, Rabuck A D, Raghavachari K, Foresman J B, Ortiz J V, Cui Q, Baboul A G, Clifford S, Cioslowski J, Stefanov B B, Liu G, Liashenko A, Piskorz P Komaromi I, Martin R L, Fox D J, Keith T, Al-Laham M A, Peng C Y, Nanayakkara A, Challacombe M, Gill P M W, Johnson B, Chen W, Wong M W, Gonzalez C and Pople J A Gaussian03 Gaussian, Inc.: Wallingford, CT 2004

[14] Becke A D 1988 *Phys. Rev.* A **38** 3098

[15] Lee C, Yang W and Parr R G 1988 *Phys. Rev.* B **27** 785

[16] Wadt W R and Hay P J 1985 *J. Chem. Phys.* **82** 284

[17] Han J G and Shi Y Y 2001 *Chem. Phys.* **266** 33

[18] Han J G and Hagelberg F 2001 *Chem. Phys.* **263** 255

[19] Han J G and Hagelberg F 2001 *J. Mol. Struct.*: *THEOCHEM* **549** 165

[20] Han J G, Xiao C Y and Hagelberg F 2002 *Struct. Chem.* **13** 173

[21] Ren Z Y, Li F, Guo P and Han J G 2005 *J. Mol. Struct.*: *THEOCHEM* **718** 165

[22] Citra A and Andrew L 1999 *J. Phys. Chem.* A **103** 3410.

[23] Gingerich K A and Cocke D L 1972 *J. Chem. Soc. Chem. Commun.* **1** 536

[24] Li S, Van Zee R J, Weltner W J and Raghavachari K 1995 *Chem. Phys. Lett.* **243** 275

[25] Xiao C and Hagelberg F 2000 *J. Mol. Struct.*: *THEOCHEM* **529** 241